Proceedings of the 3rd Croatian Conference on Earthquake Engineering - 3CroCEE
19–22 March 2025, Split, Croatia

DOI: https://doi.org/10.5592/CO/3CroCEE.2025.144

APPLICATION OF THE NEW EUROCODE 8 TO THE SEISMIC ASSESSMENT OF AN EXISTING BUILDING IN ZAGREB

Andrea Brunelli [(1)], Silvia Pinasco [(1)], Serena Cattari [(1)], Sergio Lagomarsino [(1)]

(1) Department of Civil, Chemical and Environmental Engineering, University of Genoa, Italy

andrea.brunelli@edu.unige.it, silvia.pinasco@edu.unige.it, serena.cattari@unige.it, sergio.lagomarsino@unige.it

Abstract

The second-generation of Eurocode 8 (EC8) has reached an advanced stage of development and some validations have already been made. With reference to the seismic assessment of existing masonry buildings, the nonlinear static analysis is the main pathway to proceed, but linear analysis may also be used, both in terms of strength (q-factor approach) and deformation. Even if some of these methods are already in use within some existing codes, including the Italian one, the EC8 draft incorporates new assumptions and refined criteria. These updates specifically address the verification and modelling criteria for masonry elements (piers and spandrels); in particular, spandrels may be explicitly modelled or considered indirectly. In the context of nonlinear static analysis, new criteria are outlined for defining the equivalent single-degree-of-freedom system and the limit states conditions. The implications of these newly proposed methods are investigated, with reference to an existing building in downtown Zagreb, constructed in the early twentieth century and representing a significant piece of the built heritage in the town. Buildings of this type suffered extensive damage after the earthquakes in 2020, especially within Zagreb's historic centre. The selected URM building has a rectangular floor plan and five-stores in elevation, providing a suitable case study to examine the effectiveness and adaptability of the EC8 methodologies in addressing the vulnerabilities of heritage masonry buildings under seismic actions.

Keywords: seismic assessment, linear and nonlinear static analyses, seismic verifications

1. Introduction

The activities in Croatia following the two earthquakes in 2020 (the first in Zagreb on March 22, with a magnitude of 5.3 M_w, and the second in Petrinja on December 29, with a magnitude of 6.4 M_w) have highlighted that the seismic vulnerability of the exposed building stock is a relevant issue. These earthquakes caused widespread damage to buildings in Zagreb, and particularly in Petrinja, as well as in the nearby towns of Glina and Sisak (see [1,2,3]).

The historic centre of Zagreb features a very old building stock, consisting mainly of unreinforced masonry (URM) buildings ranging from three to five stories, predominantly constructed after the 1880 Zagreb earthquake (see [4]) within 'row' aggregates. Issues contributing to the inadequate seismic design of these buildings include flexible timber floors that lack the "box-like" behaviour, poor material quality (especially mortar), poorly constructed spandrels affecting wall connections, inadequate connections between load-bearing walls and the horizontal diaphragms, and uneven stiffness distribution in the vertical elements [5].

This paper examines the in-plane seismic response of a five-story URM building in Zagreb. Specifically, the study focuses on the verification of this building according to the provisions of the draft Eurocode 8-3 [6]. Three primary verification approaches from the EC8-3 draft are compared: (1) linear static analysis (LSA) with the design spectrum, reduced by the behaviour factor q, for the force-based approach, (2) LSA with the displacement-based approach, and (3) non-linear static analysis (NLSA). A numerical model was developed for both the linear and non-linear static analyses. The model was created using the equivalent-frame modelling approach, implemented in the 3Muri software [7].

Proceedings of the 3rd Croatian Conference on Earthquake Engineering - 3CroCEE
19–22 March 2025, Split, Croatia

DOI: https://doi.org/10.5592/CO/3CroCEE.2025.144

2. Case study

The case study focuses on a representative residential building located in Zagreb's Lower Town, a historic area characterized by a distinctive urban fabric composed of row buildings in aggregate. The urban development of Zagreb's Lower Town was largely shaped by the reconstruction efforts following the earthquake of 1880. The area features a dense grid layout, adapted to pre-existing obstacles, resulting in irregularly shaped blocks that are predominantly rectangular or trapezoidal. Row aggregates, which are a defining characteristic of this area, typically consist of five or more adjacent buildings on each side, with spanning lengths between 50 and 150 meters.

These row buildings, constructed from the late 19th century until the early 20th century, do not share common walls but are built in close proximity, with no gaps or seismic expansion joints between them. Structural configurations within these aggregates vary depending on the building's position, whether located within a row or at the corner of an aggregate. Buildings situated within the row are the most common typology, and their structural system relies heavily on longitudinal load-bearing walls, while the transverse direction often lacks sufficient structural elements, except for staircase walls and the two peripheral transverse walls [8].

The specific building analyzed herein, constructed in 1908, is part of a row building aggregate, which is typical in Zagreb's Lower Town. It has a rectangular plan measuring 19,20 x 12,35 meters, a basement, a ground floor, three upper floors, and an attic (Figure *1*). The total height of the building is 22,70 meters, with floor heights of 3 meters for the basement, 3,85 meters for the ground and upper floors, and 4,20 meters for the attic. Load-bearing walls are constructed of solid bricks, with wall thickness ranging from 75 cm at the base to 30 cm at higher levels, reflecting a gradual reduction in thickness with height [9]. Notably, the building does not include reinforced concrete ring beams to connect walls at the level of horizontal diaphragms. The basement's horizontal structure consists of shallow brick barrel vaults supported by steel beams, while the upper floors utilize wooden beam systems filled with rubble material. The beams are oriented transversely, resting on the facade and the central longitudinal wall. This configuration results in greater stiffness in the longitudinal direction, while the transverse direction is structurally weaker due to the lack of adequate connections between floors and walls [8].

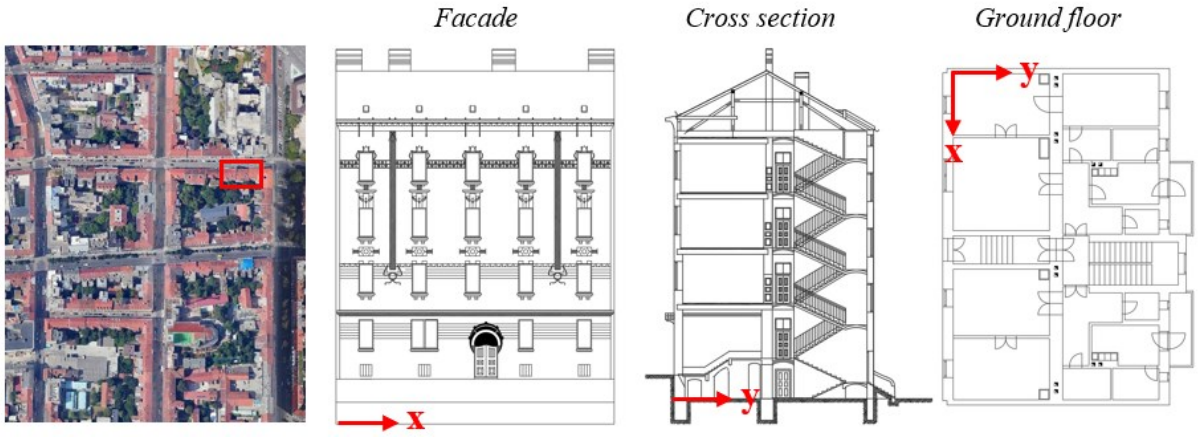

Figure 1. Aggregate to which the analyzed building belongs and a graphical representation of the main façade, the transversal vertical section, and the ground floor plan [8].

The building was modelled according to the equivalent frame approach, by using the program Tremuri [7]. The model is the same used in [8], where the aggregate effect was investigated. In this paper, for the sake of simplicity, the building is assumed as isolated (or the interaction with adjacent buildings, which are structurally independent, is neglected). The geometric model and 3D equivalent frame model are shown in Fig. 2.

The mechanical characteristics assumed are in accordance with the mean values of Table C.1 in Annex C of [6] for *solid clay brick masonry and lime mortar*. The mechanical elastic properties are reported in Table 1: E and G are the Young and shear modulus, w is the specific weight, f_m is the

DOI: https://doi.org/10.5592/CO/3CroCEE.2025.144

compressive strength, f_t is the diagonal tensile strength, f_{v0} is the shear strength in the absence of vertical load and f_b is the normalized compressive strength of the units (as defined in [10]).

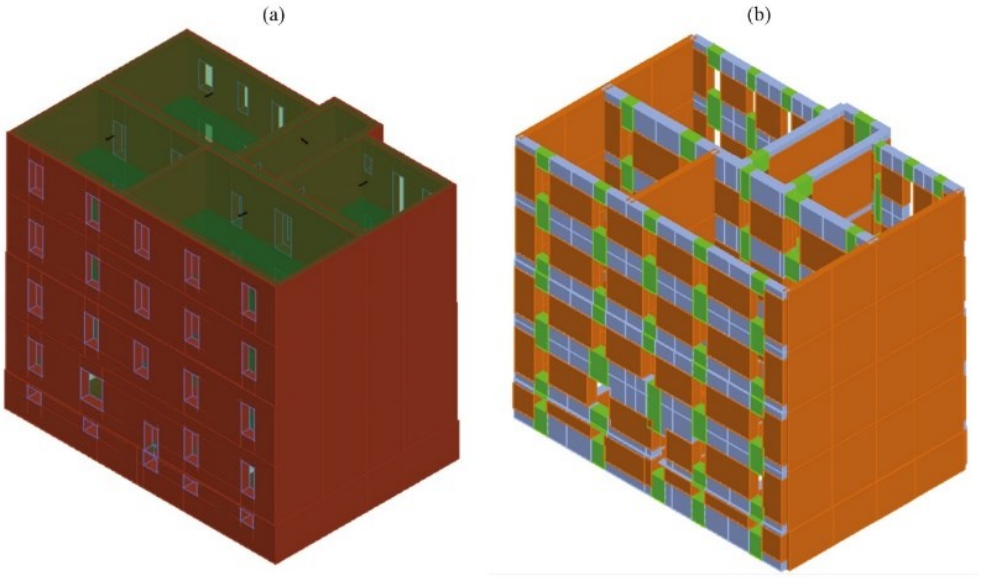

Figure 2. (a) Geometrical model and (b) 3D equivalent frame model of case study,

Table 1 – Mechanical properties

E [MPa]	G [MPa]	w [kN/m^3]	f_m [MPa]	f_t [MPa]	f_{v0} [MPa]	f_b [MPa]
1500	500	18	3.4	0.114	0.160	10

The flexural modulus is defined in accordance with [10]: for piers (in orange in the Fig. 2b) the Young modulus is reduced by multiplying the elastic value by 0.5, G by 0.35. For spandrels (in green in Fig. 2b) both moduli are reduced by multiplying the elastic values by 0.25, as proposed in EC8-1.2 [11]. The Knowledge Level (KL) is defined in function of three categories: Geometry (KLG), construction Details (KLD) and Material properties (KLM). The first two parameters are used to reduce drift in terms of drift capacity, and the third to reduce resistance. For all the three categories KL2 has been assumed, consistently with the guidance in chapter 5.4 of EC8-3.
The reference spectral acceleration is defined as S_α=2.45 m/s^2 consistent with Annex A of EC8-1.1 [12]. As defined in [8], the soil is classifiable as type C, in according with EC8-1.1, being $V_{S,30}$ equal to 275 m/s. Therefore, the site amplifications proposed in EC8-1.1 were considered, while a flat soil was assumed.

3. Seismic assessment in accordance with second-generation of EC8 part 3

In this section, a brief description of the new features of EC8-3 and the subsequent results obtained for the case study under consideration are given. The seismic action is defined using the criterions defined in the next generation of Eurocode 8 (see [12,13]), associated with the site's hypotheses described in previous section at 475 years return period for Significant Damage (SD) verification, and also 975 years for Near Collapse (NC) verification, in the case of Static Non-Linear analyses.

3.1. Linear static analysis with the reduced spectrum for the Force-based approach

This analysis reduces the elastic spectrum of a q-factor equal to 1.5 for masonry buildings.
The estimation of the fundamental period (T_1) of the building, for each direction, may be calculated with Eq. (1).

Proceedings of the 3rd Croatian Conference on Earthquake Engineering - 3CroCEE
19–22 March 2025, Split, Croatia

DOI: https://doi.org/10.5592/CO/3CroCEE.2025.144

$$T_1 = 2\sqrt{\frac{\Sigma m_i s_i^2}{\Sigma m_i s_i}} \tag{1}$$

where s_i is the horizontal displacement at node i obtained by applying horizontal acceleration equal to the gravity and m_i is the mass at node i. Therefore, the execution of a preliminary linear analysis to estimate the fundamental period is required. A new aspect respect to previous Eurocode [11] or other present codes (for example the Italian code [14]) is the distribution of forces to be applied to the structure; the recommended distribution is hence defined in Eq. (2).

$$F_i = F_b \frac{s_i m_i}{\Sigma s_j m_j} \tag{2}$$

where s_i and m_i are the same displacements and masses used for the calculation of fundamental periods and F_b is the total seismic equivalent force (see [12]), evaluated by the acceleration response spectrum at the estimated fundamental period T_1 in the direction of analysis. The point of application of the forces F_i considers a minimum eccentricity requirement, whose recommended value is equal to 5% of the corresponding length of the building including the natural eccentricity between centre of mass and centre of stiffness varies among the stories, if the natural eccentricity is lower than the minimum eccentricity.
The safety check to be performed on the masonry elements is defined by Eq. (3).

$$\gamma_{Sd}\, V \leq \frac{V_R}{\gamma_{Rd}} \tag{3}$$

where γ_{Sd} is the partial factor depending on the present state of the building, which should be assumed equal to 1 in the case of undamaged structures, γ_{Rd} is the partial factor in the resistance, V is the shear force from the analysis at the SD limit state, V_R is the strength defined as minimum among the possible failure modes:

- Failure in flexure

$$V_{R,f} = \frac{DN}{2H_0}\left(1 - \frac{N}{Dtf_m\eta_f}\right) \tag{4}$$

where D is the length in the case of piers and depth for spandrels, t is the thickness of the masonry element, H_0 is the distance between the section where the flexural resistance is attained and the contraflexure point, N is the compression value obtained from the analysis, f_m is the mean compressive strength of masonry and η_f is assumed equal to 0.85. In this case γ_{Rd}=1.85 for KLM equal to 2.

- Failure by shear sliding

$$V_{R,s}=\min\begin{cases} D't\left(f_{v0} + \dfrac{\mu N}{D't}\right) \\ 0.065\, f_b D't \end{cases} \tag{5}$$

where D' is the depth of compressed area at the end section of the pier, t is the pier thickness, μ is the masonry friction coefficient, which is assumed equal to 0.5, f_{v0} is the shear strength in the absence of vertical load, f_b is the normalized compressive strength of the units in agreement with [10]. In this case γ_{Rd}=1.50 for KLM equal to 2.

- Failure by diagonal cracking

Proceedings of the 3rd Croatian Conference on Earthquake Engineering - 3CroCEE
19–22 March 2025, Split, Croatia

DOI: https://doi.org/10.5592/CO/3CroCEE.2025.144

$$V_{R,d}=\min\begin{cases}\frac{Dt}{\mathrm{b}}\left(\frac{f_{v0}}{1+\mu_i\Phi}+\frac{\mu_i N}{(1+\mu_i\Phi)Dt}\right)\\ \frac{Dt}{\mathrm{b}}\frac{0.1f_b}{2.3}\sqrt{1+\frac{N}{0.1Dtf_b}}\end{cases} \tag{6}$$

where D and t are the dimensions of pier or spandrel, f_{v0} is the shear strength in the absence of vertical load, f_b the normalized compressive strength of the units in agreement with [10], $b = {}^{H}/_{D}$ (but not greater than 1.5 and not lower than 1), μ_i is the local friction coefficient which is assumed equal to 0.6, Φ is the interlocking coefficient assumed equal to 0.5. In this case γ_{Rd}=1.55 for KLM equal to 2.

The results of the four linear static analyses (X or Y directions, positive or vertical) are shown in Table 2 and Table 3. The most punishing verification is that associated to shear sliding, especially in the top section of piers at the last level. This depends on the very low level of compression (axial force), which in a few cases from the equivalent frame model becomes a tensile axial force. Also, the verification of the spandrels is problematic (see Table 4).

Table 2 – Capacity/demand ratios for top and bottom section of piers and percentage of elements verified in case of flexural or shear sliding failure

	Top section of piers				**Bottom section of piers**			
	+100%F_x -30%F_y	**-100%F_x +30%F_y**	**+100%F_y -30%F_x**	**-100%F_y +30%F_x**	**100%F_x -30%F_y**	**-100%F_x +30%F_y**	**100%F_y -30%F_x**	**-100%F_y +30%F_x**
Verified cases	100%	99%	99%	98%	100%	100%	100%	100%
$min\left(\frac{V_{R,f}}{\gamma_{Rd}V}\right)$	1	1	1	1	2.91	56.5	106	104
Verified cases	82%	88%	79%	78%	89%	91%	84%	85%
$min\left(\frac{V_{R,s}}{\gamma_{Rd}V}\right)$	0.01	0.01	0.04	0.03	0	0.04	0.07	0.08

Table 3 – Capacity/demand ratios for top and bottom section of piers and percentage of elements verified for diagonal cracking

	+100%Fx -30%Fy	**-100%Fx +30%Fy**	**+100%Fy -30%Fx**	**-100%Fy +30%Fx**
Verified cases	96%	98%	99%	99%
$min\left(\frac{V_{R,d}}{\gamma_{Rd}V}\right)$	0.76	0.91	0.9	0.71

Table 4 – Capacity/demand ratios for spandrels and percentage of elements verified

	+100%Fx -30%Fy	**-100%Fx +30%Fy**	**+100%Fy -30%Fx**	**-100%Fy +30%Fx**
Verified cases	26%	31%	70%	66%
$min\left(\frac{V_{R,d}}{\gamma_{Rd}V}\right)$	0.18	0.16	0.21	0.24

Therefore, the building is not verified by this procedure with the equivalent frame model. This result is similar to that already observed for the design of new masonry buildings with EC8-1.2 [15]. To

Proceedings of the 3rd Croatian Conference on Earthquake Engineering - 3CroCEE
19–22 March 2025, Split, Croatia

DOI: https://doi.org/10.5592/CO/3CroCEE.2025.144

overcome the critical issues of force-based verification by linear analysis, that are in masonry piers with very low strength but also low seismic demand, an attempt was made by modifying the numerical model by not explicitly modeling the last level spandrels, thus neglecting the contribution of the spandrels at the upper level (option 2). To this aim, the constraint at the top of the piers at the last level in the upper section has been assumed as a hinge, thus having a zero-bending moment and so the top section of the last level piers (the critical section in previous analyses) is entirely compressed (D'=D).

In Table 5 and Table 6 the results for the three typology of failure are reported; for the sake of brevity, the verification of the spandrels is not reported, because the results are similar to those shown in Table 4. The most punishing verification is always the shear sliding, although it improves over the previous configuration, the flexural verification is satisfied in almost all sections of the piers.

Anyway, even if the modified structural model reduces the number of critical piers, this model is found to be unverified at the site under consideration using LSA with the Reduced spectrum for the Force-based approach.

Table 5 – Capacity/demand ratios for top and bottom section of piers and percentage of elements verified in case of flexural or shear sliding failure (option 2 –spandrels neglected at the upper level)

	Top section of piers				**Bottom section of piers**			
	+100%Fx -30%Fy	**-100%Fx +30%Fy**	**+100%Fy -30%Fx**	**-100%Fy +30%Fx**	**100%Fx-30%Fy**	**-100%Fx +30%Fy**	**100%Fy-30%Fx**	**-100%Fy +30%Fx**
Verified cases	100%	100%	100%	100%	100%	100%	99%	100%
$min\left(\frac{V_{R,f}}{\gamma_{Rd}V}\right)$	1	1	1	1	1	1	0.86	1
Verified cases	91%	92%	87%	86%	88%	87%	85%	84%
$min\left(\frac{V_{R,s}}{\gamma_{Rd}V}\right)$	0.01	0.11	0.04	0.07	0.03	0	0.01	0.03

Table 6 – Capacity/demand ratios for top and bottom section of piers and percentage of elements verified for diagonal cracking (option 2 –spandrels neglected at the upper level)

	+100%Fx -30%Fy	**-100%Fx +30%Fy**	**+100%Fy -30%Fx**	**-100%Fy +30%Fx**
Verified cases	97%	99%	99%	99%
$min\left(\frac{V_{R,d}}{\gamma_{Rd}V}\right)$	0.76	0.92	0.81	0.72

3.2. Linear static analysis with the Displacement-based approach

This verification is allowed in [6] for existing masonry buildings, while it cannot be performed for new masonry buildings, according to EC8-1.2 [11]. The verification consists of performing a linear static analysis, as described in the previous chapter, with the elastic response spectrum not reduced by the q-factor. The purpose of this verification is to check that the deformation demand is lower than the deformation capacity in elements not verified in strength. Specifically, the same verification in terms of strength as described in the previous chapter is performed, and for the unverified elements a verification in deformation is performed using Eq. (7).

$$\gamma_{Sd}\, f_{SD}\theta \leq \frac{\theta_{SD}}{\gamma_{Rd}} \tag{7}$$

Proceedings of the 3rd Croatian Conference on Earthquake Engineering - 3CroCEE
19–22 March 2025, Split, Croatia

DOI: https://doi.org/10.5592/CO/3CroCEE.2025.144

where θ is the deformation demand drift ratio from the analysis at the SD limit state, γ_{Sd} is equal to 1 in a undamaged structure, γ_{Rd} is the partial factor in the resistance, in terms of drift capacity, for the several damage mechanisms defined in the previous section, and f_{SD} is defined in Eq. (8).

$$f_{SD} = u_{LS}\left[1 + \left(\frac{1-u_{LS}}{u_{LS}}\right)\frac{T_C}{T_1}\right] \geq 1 \tag{8}$$

where u_{LS} is equal to 0.33 being a SD verification (otherwise it would have been 0.25 for NC), T_1 the fundamental period of the building and T_C the characteristic period of the response spectrum.
This verification procedure may be used if the ratio $\rho_{max}/\rho_{min} \leq 2.5$, where $\rho = \frac{V_{Ed}}{V_{Rd}}$ in all critical zones of unverified piers. The θ_{SD} and γ_{Rd} (for KLM=2) are defined in EC8-3 in function of the typology of damage as shown in Table 7.

Table 7 – Displacement capacity and partial factor γ_{Rd} for each typology of damage

Flexure		**Shear sliding**		**Diagonal cracking**	
θSD [%]	γ_{Rd}	**θSD [%]**	γ_{Rd}	**θSD [%]**	γ_{Rd}
(1-ν)	1.85	0.5	1.50	0.6	1.55

with $\nu=\sigma_0/f_m$

This linear static analysis has been made by using the model that neglects the contribution of the last level spandrels (option 2), to limit the number of critical elements. Then, the value of ρ_{max}/ρ_{min} was calculated for all elements not verified with the equation of section 3.1 to assess whether this verification is applicable.
Table 8 shows the calculated ρ_{max}/ρ_{min} values for the four analyses. As shown in section 3.1, the shear sliding failure is the most punitive; in fact, it is observed that considering this verification in the calculation of ρ_{max}/ρ_{min}, this ratio is much higher than the limit imposed by [6]. Consequently, linear static analysis with Displacement-based approach would not be applicable. It should be pointed out that practically ρ_{max}/ρ_{min} coincides with ρ_{max}, as ρ_{min} is usually slightly larger than 1.

Table 8 – ρ_{max}/ρ_{min} for the four analyses in two cases: with and without the shear sliding failure

	+100%Fx -30%Fy	**-100%Fx +30%Fy**	**+100%Fy -30%Fx**	**-100%Fy +30%Fx**
With shear sliding failure	76.72	33.68	97.19	118.90
Without shear sliding failure	1.83	1.53	2.24	2.46

Analyzing in detail the results for the critical piers under shear sliding verification, it is observed that these are located not only at the top floor being lightly loaded, but also where a significant flange effect is activated by the equivalent frame model. Fig. 3 shows some cases of piers (in black square) where the ρ_{max}/ρ_{min} value is very large, and this occurs because, in the equivalent frame model, piers of two intersecting walls are perfectly connected, forming a T section in which the flange or the web result unloaded. In particular, in Figure 3 the perimetral transversal wall and half of the back façade are shown (see Figure 2); the pushover analysis is along the transversal direction, and elements 195, 200 and 210 resulted unloaded because connected to elements 4, 8 and 16 of the orthogonal wall, respectively (please note that they are connected to nodes 8, 9 and 11; analogously, element 13 in the transversal wall is unloaded because strictly connected through node 5 to the main façade.
To overcome this issue, the equivalent frame model could be modified, by vertically disconnecting the orthogonal piers, to verify each pier as independent and limit the redistribution of axial forces.
Anyway, with the aim of understanding the potential of linear static analysis with displacement-based verification, the verification of deformation capacity (see Eq. (7)) was considered even if ρ_{max}/ρ_{min}

DOI: https://doi.org/10.5592/CO/3CroCEE.2025.144

is larger than 2.5. Table 9 shows the capacity-demand ratios in terms of deformation and all elements are found to be verified, even where the verification is largely unsatisfied in terms of strength.
Therefore, while ASL with q-factor is very punitive and the method is practically unusable, the verification in terms of deformation is not very demanding even where the resistance is very low.

Table 9 – Capacity/demand ratios in deformation in each four analyses

	+100%Fx -30%Fy	-100%Fx +30%Fy	+100%Fy -30%Fx	-100%Fy +30%Fx
θ_{Rd}/θ_{Ed} min	1.374	1.438	1.002	1.039

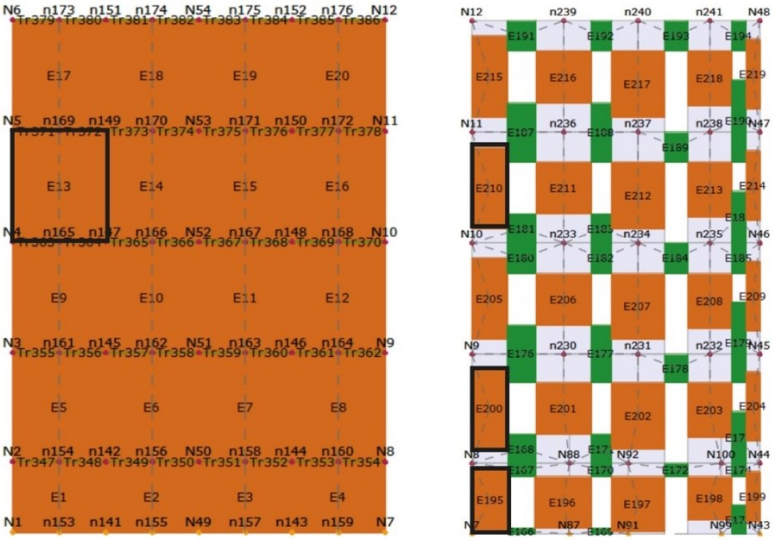

Figure 3. Example of piers in black square that fail in terms of strength due to a relevant flange effect.

3.3. Non-Linear static analysis

The verification with NLSA for building with stiff diaphragms is done using a triangular pattern based on lateral forces that are proportional to masses, considering an inverted profile in elevation (as other actual code e.g. [14]). This load pattern is preferred to the one obtained by modal analysis, which in the absence of a rigid diaphragm usually presents a limited mass participation in each mode, to avoid that only few masonry walls are loaded.
The ultimate drifts are $\theta_u=4/3\theta_{SD}$. For regular masonry piers, the force reduction corresponding to θ_u, for flexure, is assumed to be 10% of shear resistance, for spandrels the reduction is 20%. For shear sliding the reduction is in function of the compression level. Finally for diagonal cracking the reduction is for piers 50%, for spandrels 90%. The values of θ_{SD} are reported in Table 7.
The definition of the bilinear curve of the equivalent single degree of freedom (SDoF) system is done with the procedure described in [12] that recommends the adoption of a stiffness of the SDoF system equal to the secant stiffness, whereas the allowed yield strength is obtained through the equivalence of areas up to the ultimate point.
The definition of displacement capacity (d_u) of the SDoF system at the NC limit state depends on the first of three criteria:

a) the total lateral resistance (base shear) has dropped below 80% of the peak resistance of the building.
b) the damage level associated with the drift θ_{NC} is reached in all piers at any level of any masonry walls.
c) one member has researched a drift ratio corresponding to 1.5 times that corresponding to the NC damage.

DOI: https://doi.org/10.5592/CO/3CroCEE.2025.144

The d_u, defined as minimum of the three conditions, is reduced with a factor equal to 1.8 being the KL equal to 2. The characteristic displacement is the average displacement among those of different walls, weighed by the corresponding seismic masses, because the diaphragms are stiff but not rigid. Instead, the displacement capacity at the SD limit state is defined as the mean value between $d_{u,NC}$ (d_u of the SDoF system at the NC limit state as described in previous section) and d_y. Also in this case, the SD limit state is reduced with factor equal to 1.8 being the level knowledge equal to 2.

Table 10 shows the values of the capacity/demand ratio (in terms of displacements) obtained for the four nonlinear static analyses, in the case of the SD and NC limit state. At NC limit state, the verification is largely satisfied for X direction, while are barely verified in the Y direction. On the contrary, at SD limit state is not verified (0.913) in the Y direction. As an example, Fig. 4 shows the capacity curves (pushover in black and equivalent bilinear in red) for the analysis in the +X and +Y direction with the SD and NC thresholds (in the first case the displacement capacity after the application of γ_{Rd} factors is also shown with a light blue dot, the second with blue dot). The spectra are in dashed line for ND (T_R=795 years), in light blue, and for SD state limit (T_R=475 years), in blue.

In Fig. 4a and b it can be seen how the ultimate NC displacement is associated with condition (a), equally is the case in the other two analyses not shown, at a slightly larger displacement condition (c) is triggered, while condition (b) is never triggered and is not, at least for this case study, significant. Fig. 4a shows how the target (the cross) at both SD and NC is less than d_u, while in the +Y analysis (Fig. 4b) it is verified only at the NC limit state. The verification at SD is more punitive than at NC in the case where the bilinear plateau length (distance between d_y and $d_{u,NC}$) is big since it is possible to take advantage of the increase in drift at NC compared with that at SD value.

Table 10 – Values of capacity/demand ratio (in terms of displacements) for each analysis

	+X	-X	+Y	-Y
NC limit state	1.782	1.602	1.001	1.097
SD limit state	1.420	1.296	0.926	0.913

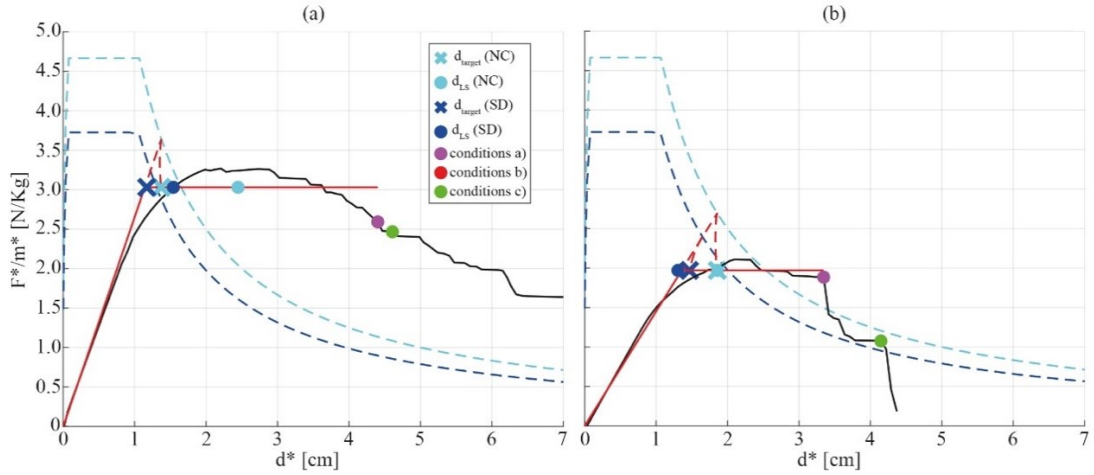

Figure 4. (a) Capacity curve and elastic response spectrum (return period 475 and 975 years) for analysis +X and (b) for +Y.

4. Conclusions

By considering a five-story URM building in Zagreb's Lower Town, built in the early 20th century, three verification procedures for the seismic assessment of existing masonry buildings have been investigated, according to the rules proposed in the current draft of the new Eurocode 8-3 [6]. In particular, it emerges that results can differ even considerably by passing from linear to non linear methods, and from force-based to displacement-based approaches.

It is confirmed how the LSA with the q-factor (force-based approach) is particularly punitive for

DOI: https://doi.org/10.5592/CO/3CroCEE.2025.144

masonry buildings in that even in medium hazard sites such as the one analyzed. This is due to the assumption that verification is in local terms, that is it fails even if the critical condition is attained only in one masonry element. Within the different failure mechanisms for masonry piers, particularly punitive is the shear sliding verification, which is requested only for regular masonry piers.
On the contrary, LSA with unreduced response spectrum and verification in deformation (displacement-based approach) appears to be an effective procedure to assess the seismic behaviour at SD limit state. However, in the present formulation the condition that allows the applicability of the method only when the overcoming in terms of strength is below 2.5 limits the large applicability of this method. Particularly problematic in this case is the verification of elements with low axial force, especially with reference to shear sliding failure. Therefore, for LSAs, it is recommended to make models in which spandrels are not explicitly modeled, especially on the top level. In addition, a critical issue is related to the use of linear analysis in building modelled by the equivalent frame approach because the significant redistribution of generalized forces between masonry elements due to the so-called flange effect. A possible approach to consider the flange effect in equivalent frame model was proposed by [16].
Finally, NLSA turns out to be an effective approach to assess existing masonry buildings, in particular when the verification is made in global terms, by checking the ultimate displacement capacity, instead to check the attainment of drift capacity in any single masonry element. In the specific case study, NC limit state is verified, while SD limit state is slightly overcome.

5. References

[1] Atalić, J., Demšić, M., Baniček, M., Uroš, M., Dasović, I., Prevolnik, S., Kadić, A., Šavor Novak, M., Nastev, M. (2023): The December 2020 magnitude (Mw) 6.4 Petrinja earthquake, Croatia: seismological aspects, emergency response and impacts. *Bulletin of Earthquake Engineering* **21**, 5767–5808, https://doi.org/10.1007/s10518-023-01758-z.

[2] Pinasco, S., Cattari, S., Lagomarsino, S., Demšić, M., Novak, M.S., Uroš, M. (2023): Numerical investigation on the seismic response of an unreinforced masonry residential building hit by Zagreb earthquake in 2020. *2nd Croatian Conference on Earthquake Engineering*, Zagreb, Croatia.

[3] Moretić, A., Chieffo, N., Stepinac, M., Lourenço, P.B. (2022): Vulnerabilit assessment of historical building aggregates in Zagreb: implementation of a macroseismic approach, *Bulletin of Earthquake Engineering*, ***0123456789***, https://doi:10.1007/s10518-022-01596-5.

[4] Šavor Novak, M., Uroš, M., Atalić, J., Herak, M., Demšić, M., Baniček, M., Lazarević, D., Bijelić, N., Crnogorac, M., Todorić, M. (2020): Zagreb earthquake of 22 March 2020-preliminary report on seismologic aspects and damage to buildings. *J Croatian Assoc Civil Eng*, **72** (10),843–867, https://doi.org/10.14256/JCE.2966.2020.

[5] Atalić, J., Uroš, M., Šavor Novak, M., Demšić, M., Nastev, M. (2021): The Mw5.4 Zagre (Croatia) earthquake o March 22, 2020 impacts and response. *Bulletin of Earthquake Engineering*, **19** (9), 3461-3489, https://doi.org/10.1007/s10518-021-011:17-w.

[6] CEN (2023): prEN 1998-1-2. Eurocode 8 - Design of structures for earthquake resistance - Part 1-2: Buildings, April 2023, Comité Européen de Normalisation, Brussels.

[7] Lagomarsino, S., Penna, A., Galasco, A., Cattari, S. (2013): TREMURI program: an equivalent frame model for the nonlinear seismic analysis of masonry buildings. *Engineering Structures*, **56**, 1787-1799, https://doi.org/10.1016/j.engstruct.2013.08.002.

[8] Pinasco, S., Demšić, M., Pilipović, A., Novak, M.S., Uroš, M., Lagomarsino, S., Cattari, S. (2025): Seismic fragility assessment of existing masonry buildings in aggregate located in Zagreb. *Bulletin of Earthquake Engineering (*submitted).

[9] Demšić, M., Pinasco, S., Pilipović, A., Cattari, S., Lagomarsino, S., Šavor Novak, M.S., Uroš, M. (2024): Development of fragility curves of masonry buildings build in a regular row aggregate. *18th World Conference on Earthquake Engineering*, 30 June - 5 July 2024, Milan, Italy.

DOI: https://doi.org/10.5592/CO/3CroCEE.2025.144

[10] CEN (2021): prEN 1996-1-1. Eurocode 6 - Design of masonry structures - Part 1-1: General rules for reinforced and unreinforced masonry structures, October 2021, Comité Européen de Normalisation, Brussels.

[11] CEN (2023): prEN 1998-1-2. Eurocode 8 - Design of structures for earthquake resistance - Part 1-2: Buildings, April 2023, Comité Européen de Normalisation, Brussels.

[12] CEN (2023): prEN 1998-1-1. Eurocode 8 - Design of structures for earthquake resistance - Part 1-1: General rules and seismic action, June 2023, Comité Européen de Normalisation, Brussels.

[13] Labbé, P., Paolucci, R. (2022): Developments relating to seismic action in the Eurocode 8 of next generation. In: Vacareanu, R., Ionescu, C. (eds) "*Progresses in European Earthquake Engineering and Seismology*", ECEES 2022. Springer Proceedings in Earth and Environmental Sciences. Springer. https://doi.org/10.1007/978-3-031-15104-0_29.

[14] NTC (2018) Aggiornamento delle Norme tecniche per le costruzioni. Italian Ministry of Infrastructure and Transportation, G.U. n. 42, 20 February 2018, Rome, Italy (in Italian).

[15] Lagomarsino, S., Penna, A., Cattari, S., Rota, M., Brunelli, A., Bracchi, S. (2024): Unresolved issues in the design of URM buildings: a critical review of linear and nonlinear methods. *18th World Conference on Earhquake Engineering,* 30 June – 5 July 2024, Milan, Italy.

[16] Cattari, S., Alfano, S., Lagomarsino, S. (2023): A Practice-Oriented Proposal to Consider the Flange Effect in Equivalent Frame Modeling of Masonry Buildings. *Buildings*, **13**(2), 462, https://doi.org/10.3390/buildings13020462.